

- reau of Standards Linac Internal Report No. 297, 1969 (unpublished); S. Penner, National Bureau of Standards Linac Internal Report No. 302, 1969 (unpublished).
- ¹²R. M. Sternheimer, *Phys. Rev.* **91**, 256 (1953); **103**, 511 (1956).
- ¹³J. Bergstrom, Massachusetts Institute of Technology Report No. TID-24667, 1967 (unpublished).
- ¹⁴H. Nguyen-Ngoc and J. P. Perez-y-Jorba, *Phys. Rev.* **136**, B1036 (1964).
- ¹⁵L. C. Maximon, *Rev. Mod. Phys.* **41**, 193 (1969).
- ¹⁶L. Heitler, *Quantum Theory of Radiation* (Oxford U.P., Oxford, England, 1954), 3rd ed., p. 377.
- ¹⁷L. Landau, *J. Phys. (USSR)* **8**, 201 (1944).
- ¹⁸W. Borsch-Supan, *J. Res. Natl. Bur. Std. B* **65**, 245 (1961).
- ¹⁹H. A. Bentz, *Z. Naturforsch.* **24a**, 858 (1969).
- ²⁰H. A. Bethe and J. Ashkin, in *Experimental Nuclear Physics*, edited by E. Segré (Wiley, New York, 1953), Vol. I.
- ²¹J. C. Butcher and H. Messel, *Nucl. Phys.* **20**, 15 (1960).
- ²²T. de Forest, Jr., *Nucl. Phys.* **A132**, 305 (1969).
- ²³Y.-S. Tsai, in *Nucleon Structure*, edited by R. Hofstadter and L. I. Schiff (Stanford U. P., Stanford, 1964), p. 221.
- ²⁴N. T. Meister and T. A. Griffy, *Phys. Rev.* **133**, B1032 (1964).
- ²⁵Lightbody, Jr., and Penner, see Ref. 1.
- ²⁶J. M. Wyckoff, B. Ziegler, H. W. Koch, and R. Uhlig, *Phys. Rev.* **137**, B576 (1965).
- ²⁷F. C. Barker, *Nucl. Phys.* **28**, 96 (1961).
- ²⁸B. R. Easlea, *Phys. Letters* **1**, 163 (1962).
- ²⁹D. F. Measday, A. B. Clegg, and P. S. Fisher, *Nucl. Phys.* **61**, 269 (1965).
- ³⁰K. Fukuda, *Nucl. Phys.* **A156**, 10 (1970).
- ³¹P. S. Fisher, D. F. Measday, F. A. Nicolaev, A. Kalmykov, and A. B. Clegg, *Nucl. Phys.* **45**, 113 (1963).
- ³²J. O'Connell, *Phys. Letters* **22**, 1314 (1969).
- ³³H. Morinaga, *Phys. Rev.* **97**, 444 (1955); *Z. Physik* **188**, 182 (1965).
- ³⁴S. Fallieros, B. Goulard, and R. H. Venter, *Phys. Letters* **19**, 398 (1965).
- ³⁵M. H. Macfarlane, in *Isobaric Spin in Nuclear Physics*, edited by J. D. Fox and D. Robson (Academic, New York, 1966), p. 383.
- ³⁶O. Titze, A. Goldmann, and E. Spamer, *Phys. Letters* **31B**, 565 (1970).
- ³⁷B. Goulard and S. Fallieros, *Can. J. Phys.* **45**, 3221 (1967).
- ³⁸J. S. Levinger, *Nuclear Photodisintegration* (Oxford U.P., Oxford, England, 1960).
- ³⁹E. Hayward, *Photoneuclear Reactions* (National Bureau of Standards Monograph No. 118, 1970).

PHYSICAL REVIEW C

VOLUME 4, NUMBER 5

NOVEMBER 1971

${}^3\text{He}({}^3\text{He}, 2p){}^4\text{He}$ Total Cross-Section Measurements Below the Coulomb Barrier*

M. R. Dwarakanath and H. Winkler†

California Institute of Technology, Pasadena, California 91109

(Received 25 June 1971)

Measurements of total cross sections for ${}^3\text{He}({}^3\text{He}, 2p){}^4\text{He}$ have been made for center-of-momentum energies between 80 keV and 1.1 MeV. A continuously recirculating differentially pumped gas target system was employed to minimize uncertainties in energy loss and straggling. A calorimetric device was used to integrate the beam current within the target gas. Proton angular distributions were measured at seven energies. The measured cross-section factor, $S(E)$, was fitted to a linear function of energy for $E_{\text{c.m.}} < 500$ keV:

$$S(E_{\text{c.m.}}) = S_0 + S_0' E_{\text{c.m.}},$$

where $S_0 = (5.0^{+0.6}_{-0.4})$ MeV b and $S_0' = (-1.8 \pm 0.5)$ b. The formula $S(E_{\text{c.m.}}) = S_0 + S_0' E_{\text{c.m.}} + \frac{1}{2} S_0'' E_{\text{c.m.}}^2$, with $S_0 = 5.2$ MeV b, $S_0' = -2.8$ b, and $S_0'' = 2.4$ b MeV⁻¹ gives a good representation of $S(E)$ over the entire range of energies studied here.

I. INTRODUCTION

For solar-model calculations, it is necessary to have accurate total cross sections for the reaction ${}^3\text{He}({}^3\text{He}, 2p){}^4\text{He}$ at energies well below the Coulomb barrier.¹ This reaction completes one branch of the proton-proton chain of nuclear reactions, the dominant energy-generation mechanism in certain main sequence stars such as our sun. The rate of this reaction is an important factor in determining the relative importance of the different branches of the p - p chain in the sun. In particular, the

branch terminated by the sequence ${}^7\text{Be}(p, \gamma){}^8\text{B}(e^+ \nu) - {}^8\text{Be}(\alpha){}^4\text{He}$ produces neutrinos with energies up to 14.1 MeV, and the detection of these neutrinos constitutes a direct test of solar models.² Such a test is quantitative only if the nuclear information used in the models is accurate. The cross section at 20 keV (c.m.) for the reaction ${}^3\text{He}({}^3\text{He}, 2p){}^4\text{He}$ is estimated to be about 3×10^{-13} b and thus cannot be measured directly in the laboratory. Hence, the cross section or rather the cross-section factor has to be extrapolated from measurements at higher energies. The cross-

section factor $S(E)$ is the total cross section with the dominant energy dependence factored out

$$S(E) \equiv \sigma(E) E e^{2\pi\eta}; \quad \eta = \frac{Z_0 Z_1 e^2}{\hbar v},$$

with Z_0 , Z_1 , v , and E equal to the charge numbers, the relative velocity, and the center-of-momentum energy of the interacting particles. $S(E)$ varies only slowly with energy for nonresonant processes and so is more suitable for extrapolation than the rapidly varying $\sigma(E)$.

The total cross section for ${}^3\text{He}({}^3\text{He}, 2p){}^4\text{He}$ was first measured by Good, Kunz, and Moak³ in 1953. The chief uncertainty in their measurements lies in the bombarding energy, as they employed a thick target of ${}^3\text{He}$ atoms trapped in an aluminum foil. The uncertainty in the energy is reflected as a large uncertainty in $S(E)$ through the exponential term. Bacher and Tombrello⁴ have investigated the reaction in detail for $0.5 < E_{c.m.} < 18$ MeV. At energies above the Coulomb barrier, they interpret their results as demonstrating that the reaction proceeds through the intermediate step, ${}^5\text{Li} + p$. However, a different mechanism is required to explain the different shape of the proton energy spectra at bombarding energies well below the Coulomb barrier. Thus, the data at higher energies cannot be extrapolated to the energy regions of astrophysical interest. Neng-Ming *et al.*⁵ have reported measurements in the energy region $0.25 < E_{c.m.} < 0.85$ MeV. Concurrently with the present work, Bacher and Tombrello⁶ extended their measurements to lower energies by modifying their gas-cell target system. These results will be compared in a later section.

The present work describes measurements for $0.08 < E_{c.m.} < 1.1$ MeV, and employs a new technique for rare-gas targets. It has the advantage of eliminating the entrance window for the primary beam and at the same time using limited quantities of the rare gas. Beam integration was carried out inside the gas target by a calorimetric method. The protons and α particles were identified by a ΔE - E counter telescope with a transmission gas proportional counter as the first element of the telescope. Preliminary results of this work were given earlier.⁷

II. EXPERIMENTAL APPARATUS

Singly charged ${}^3\text{He}$ ions were obtained from the California Institute of Technology 3-MV and 500-kV Van de Graaff electrostatic generators. The energy calibrations of the magnetic analyzers for the accelerated beam were checked by observing well-known (p, γ) and ($p, \alpha\gamma$) resonances with both protons and the molecular ions, HH^+

and HHH^+ . The energy of the beam from the accelerator was thus known to within ± 1 keV.

The differentially pumped gas target apparatus is shown in Figs. 1 and 2. The beam entered the target region through three canals. The main pressure drop occurred across canal A (see Figs. 1 and 2) which was 3 mm in diameter and 2 cm long. This canal connected the target chamber to a large-volume chamber A, which was pumped by a set of three Roots blowers in cascade. The output of the third Roots blower developed a sufficiently high pressure to allow recirculation of the gas. However, the gas coming out of the pumps was contaminated both by traces of oil vapor from the pumps and by air leaking into the system through small real or virtual leaks. The gas was cleaned of impurities by passing it through a zeolite adsorption trap at liquid-nitrogen temperature. The chilled gas coming out of the trap was allowed to exchange heat with the incoming gas before the gas was fed back to the target chamber, typically at a pressure of 20 Torr. The adsorber was very efficient in removing all gases and vapors except helium. The number of impurity atoms was found to be less than 1% of the number of helium atoms by observing the elastic scattering of protons from the gas target.

The pressure in chamber A was typically 0.1 Torr. This chamber was connected to another large volume, chamber B, by canal B which was 3.5 mm in diameter and 10 cm long. Chamber B was pumped by a 10-cm oil diffusion pump with its backing line connected to chamber A. This allowed the recovery of most of the gas streaming through canal B. Since the pressure in chamber B was typically 2×10^{-5} Torr, the beam pipe from the accelerator could be connected directly to this chamber through a third impedance, canal C. The gas leaking through canal C was about 1% of the total charge per hour and was not recovered. The total recirculating gas charge was approximately 500 cm^3 STP for a target pressure of 20 Torr.

The beam energy loss up to the point of entering canal A was negligibly small. In order to minimize the subsequent energy loss of the beam, canal A was positioned as close as possible to the target region. The tip of canal A was 7 mm from the center of the target chamber, thus permitting a target thickness of up to 1 cm to be used. The energy loss of the beam at the target center was about 15 keV and the uncertainty in this was only 3 keV under the most adverse conditions. An aperture, slightly smaller than the bore of canal A, was placed at the entrance of the canal; the canal therefore also served as an antiscattering baffle. The fraction of degraded beam was mea-

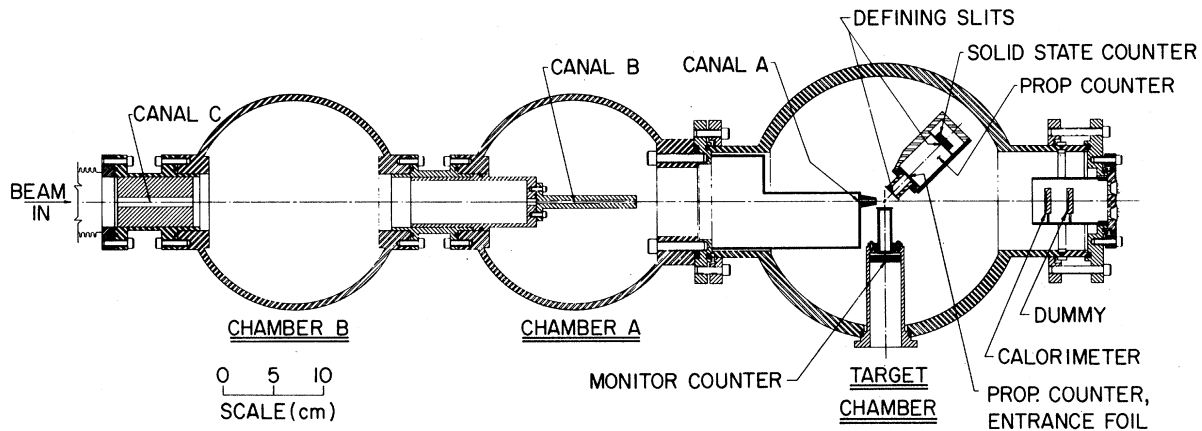


FIG. 1. A horizontal section of the differentially pumped gas target apparatus with counter telescope positioned at 45° to beam direction.

sured to be less than 0.5% for 1-MeV protons. The temperature and pressure of the gas were continuously monitored. Gas pressure could be measured accurately to ± 0.1 Torr on an aneroid gauge, the accuracy of which was previously ascertained by an absolute gauge of the McLeod type. As the gas is continuously flowing out of the target region, the temperature here is estimated to be only 1 to 3°C higher than the gas temperature at the wall of the target chamber where the

temperature was monitored. Reduction of gas pressure in the target region due to space-charge repulsion and hard collisions is not important at the target pressures and beam currents employed. This has been verified experimentally by employing beam currents differing by a factor of about 4. The gas pressure in the target region is essentially unmodified by the gas flow through the canal as the center of the target is situated several canal radii away from the end of the canal. There is

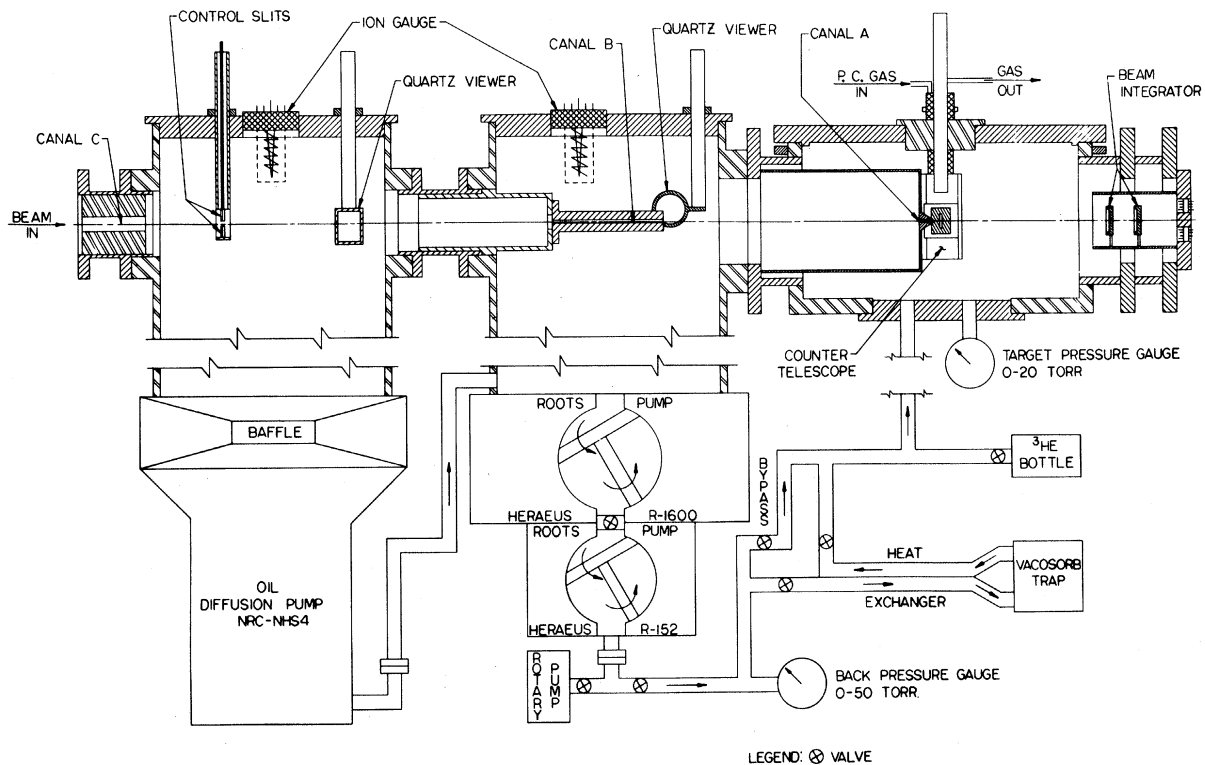


FIG. 2. A vertical section of the differentially pumped gas target apparatus with counter telescope positioned at 90° to beam direction. Only the upper part of the figure is drawn to scale.

thus an uncertainty of about 2–3% in the target density which is included in the quoted errors.

Beam integration was carried out inside the gas target by measuring the heat dissipated by the beam in a low-mass, high-conductivity metal cup called the calorimeter. The calorimeter was mechanically supported from a large flange, acting as an infinite heat sink, by means of a soldered thin stainless-steel tube constituting a well-defined heat leak. Some heat was also carried away from the calorimeter by the target gas. The heat produced by the beam in the calorimeter was measured by determining the amount of electrical energy put into a dummy of similar construction to maintain the calorimeter and the dummy at the same temperature during beam integration. The electrical energy supplied to the dummy did not exactly equal the energy put into the calorimeter by the beam because of a small departure from symmetry in the construction of the two heat leaks; however, the proportionality constant between the calorimeter and dummy was determined by supplying a measured amount of electrical energy to the calorimeter. This proportionality constant is called the calibration constant K . The number of incident particles N_B is given by

$$N_B = \frac{KW_g}{E_c},$$

where K is the calibration constant, W_g is the electric energy supplied to dummy, and E_c is the beam energy at the calorimeter. The energy loss of the beam in the gas, before hitting the calorimeter, is important in this method of beam integration. Energy losses were calculated from tables.^{8,9} The errors introduced into N_B and E , the energy at the center of the target, by uncertainties in the specific energy loss contribute to errors in $S(E)$ in opposite directions. Therefore, systematic errors in the specific energy-loss data are partially compensated in $S(E)$.

The accuracy of the calorimetric beam-integration device was checked by measuring the known¹⁰ differential cross section for ${}^{40}\text{A}(p, p){}^{40}\text{A}$ at 135° in the laboratory with proton energies below 1.8 MeV (pure Rutherford scattering). For a beam power range from 30 mW to 3 W and varying conditions of beam stability, the uncertainty in N_B was found to be less than $\pm 5\%$ for runs of 4 min or longer. A more detailed description of this beam-integration device is given elsewhere.^{11,12}

The reaction particle spectra were measured with a ΔE - E counter telescope in order to separate the protons from the α particles, both of which have continuous energy spectra from zero to the three-body end point. The transmission (ΔE) counter limits the observation of particle

spectra to energies not stopped inside it; for this reason it is desirable to use as thin a ΔE detector as possible. A gas proportional counter with a 0.6-mg/cm^2 Ni foil entrance window was used in the present experiment and the window was chosen so that it was sufficiently thick to stop the strong flux of elastically scattered ${}^3\text{He}$'s. Continuously flowing argon +5% CO_2 at a pressure of about 70 Torr was used as the proportional-counter gas and the gas multiplication factor was between 100 and 1000. The resolution of the proportional counter was adequate to separate completely protons and α particles of the same energy. The $E' \equiv (E - \Delta E)$ counter was a $1500\text{-}\mu$ silicon surface-barrier detector. Proton energies greater than 600 keV and α energies greater than 2 MeV could be measured with this telescope. The low-energy detection limit of the telescope was checked with 600-keV protons elastically scattered from argon. The counter telescope could be rotated about the center of the target chamber and the most backward angle accessible was 140° . At angles smaller than 45° the proportional-counter body eclipsed the beam path to the integrator. Absolute differential cross-section measurements were, therefore, restricted to the range of angles $45\text{--}140^\circ$. For measurements at more forward angles, a monitor counter fixed at 90° to the beam and covered with a foil to stop elastically scattered particles, was used to provide a measure of the beam intensity.

The solid angle subtended by the detector and the effective thickness of the target were defined by two apertures. The first aperture was circular with radius $a \approx 5.5$ mm and was placed directly in front of the surface-barrier detector at a distance $D \approx 80.5$ mm from the center of the target. The second aperture was rectangular with width $=2W$ and height much larger than its width, and was placed at a distance $d \approx 67.5$ mm from the circular aperture along the line joining the center of the circular aperture and the target center. The two apertures were placed perpendicular to this line. The rectangular slit was placed with its long axis perpendicular to the reaction plane. The effective product of solid angle and target thickness, for the telescope set at an angle ψ to the beam direction, is given by

$$\langle \Omega \rangle_\psi = \frac{\pi a^2 2W}{Dd} \csc \psi \left[1 + O\left(\frac{a^2}{d^2}\right) \right].$$

III. EXPERIMENTAL PROCEDURE AND ANALYSIS

The reaction particle spectra were measured using the counter telescope described above and a Nuclear Data two-dimensional pulse-height ana-

lyzer operating in a 64×64 channel configuration. Pulses from the ΔE and E' detectors were fed to the x and y analog-to-digital converters of the analyzer after amplification. A gating signal from a low-level discriminator on the E' counter pulses was required for the two-dimensional storage of a count. Particle spectra appeared on the cathode-ray-tube display of the analyzer as two nearly rectangular hyperbolas, well separated from each other and from background. The raw particle spectra were obtained by summing all the counts in the various ΔE channels corresponding to a given E' channel about the locus of the selected hyperbola. The raw particle spectra are distorted because of the energy loss ΔE , before reaching the surface-barrier counter. The true energy spectrum $N(E)dE$ was computed from the measured spectrum $N(E')dE'$ by using the relation

$$N(E)dE = \left(N(E') \times \frac{dE'}{dE} \Big|_{E'} \right) dE,$$

where $(dE'/dE)|_{E'}$ is the slope calculated from a graph of E' , the energy at the surface-barrier detector, against E , the energy at the target center. Corrected proton-energy spectra at 90° for $E_{3\text{He}} = 1.99$ and 0.19 MeV are shown in Figs. 3 and 4. The arrow at a proton energy of ~ 600 keV shows the lower limit of proton energies observed by the counter telescope. Counting statistics are

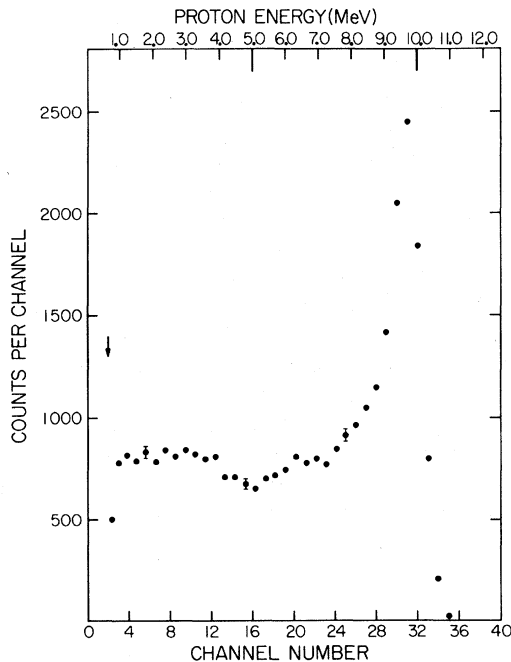


FIG. 3. Proton-energy spectrum, corrected for energy loss in the proportional-counter entrance foil, at $E_{3\text{He}} = 1.99$ MeV and $\psi = 90^\circ$. Arrow at $E_p = 0.6$ MeV indicates the low-energy detection limit of the telescope.

shown for a few representative points. The dashed curve in Fig. 4 is the spectrum calculated by assuming a statistical distribution and isotropic angular distribution in the center-of-momentum system. The peak in the proton spectrum near the three-body end point, in Fig. 3, corresponds to protons from the two-body breakup: ${}^5\text{Li} + p$. The relatively flat part of the spectrum corresponds to the breakup of ${}^5\text{Li}$ in flight and to contributions from other mechanisms. At $E_{3\text{He}} = 0.19$ MeV, the proton spectrum shows a much smaller effect of the final-state interaction in the ${}^4\text{He} + p$ system.

Total proton yields were obtained by summing all the counts in the observed spectrum. A correction for the unobserved low-energy part of the spectrum was made by assuming that the spectral shape in this narrow interval is given correctly by phase-space considerations. Though this assumption is not valid for the higher bombarding energies, it gives a rough estimate of the correction, which is itself small ($\sim 5\%$). The error in the total number of protons counted, introduced by this assumption is less than $\pm 2\%$. The differential cross section was calculated from the total proton yield $Y(E, \psi)$ at true bombarding energy E and angle ψ , by using the relation

$$\frac{d\sigma}{d\Omega} \Big|_{E, \psi} = \frac{Y(E, \psi)}{2N_B n_T \langle \Omega \rangle_\psi},$$

where n_T is the number density of the target nuclei

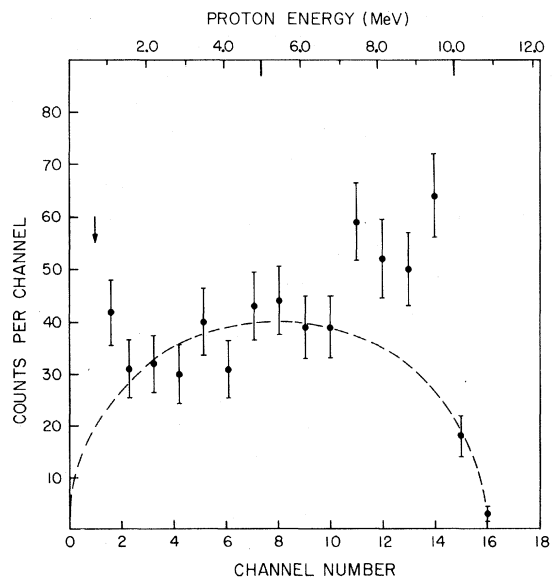


FIG. 4. Proton-energy spectrum at $E_{3\text{He}} = 0.19$ MeV and $\psi = 90^\circ$. The dashed curve shows the spectrum calculated by assuming a statistical spectral distribution and isotropic angular distribution in the center-of-momentum system.

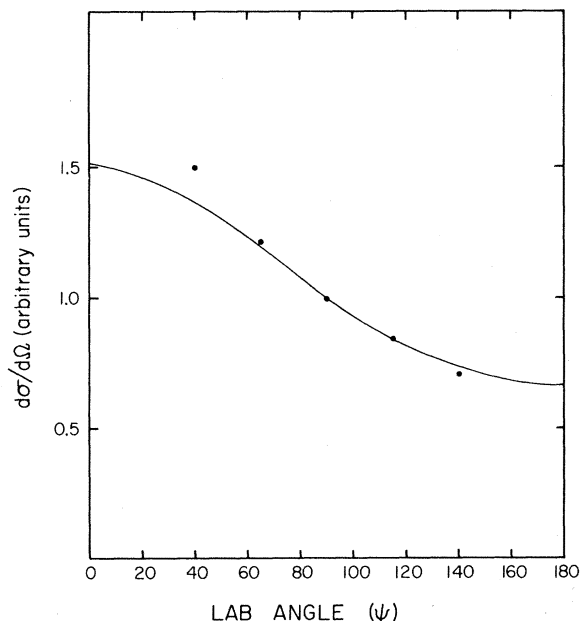


FIG. 5. Proton angular distribution in the laboratory for $E_{3\text{He}} = 2.0$ MeV. The solid curve shows the angular distribution calculated by assuming a statistical spectral distribution and isotropic angular distribution of protons in the center-of-momentum system and normalized to 1.0 at $\psi = 90^\circ$.

at the target region and all other quantities are as defined earlier. The factor $\frac{1}{2}$ appears in the cross section because two protons are released in each reaction.

Proton angular distributions were obtained at seven energies over the range of angles 20–140°

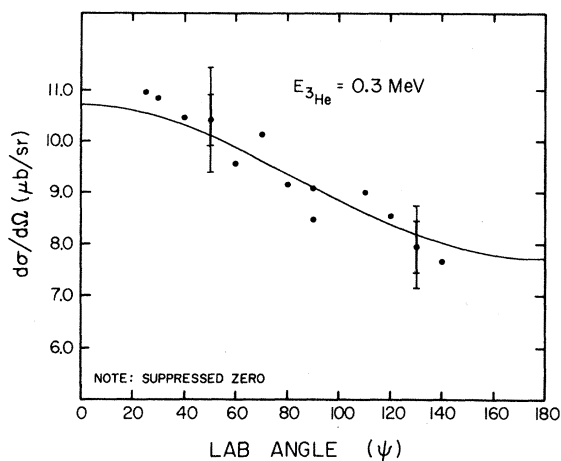


FIG. 6. Proton angular distribution in the laboratory for $E_{3\text{He}} = 0.3$ MeV. The larger error bar indicates the absolute error in the measured differential cross sections and the smaller error bar indicates the relative error between measurements at different angles. Solid curve has the same meaning as in Fig. 5.

using the monitor counter and, where possible, the beam integrator. Figures 5 and 6 show proton angular distributions at $E_{3\text{He}} = 2.0$ and 0.3 MeV. The solid curve shows angular distributions in the laboratory system, calculated under the assumption of statistical spectral distribution and isotropic angular distributions in the center of momentum. Figure 6 shows two sets of error bars at a few points. The larger bars denote the uncertainty in the absolute differential cross section while the smaller error bars give the relative errors.

The total reaction cross section was obtained by numerical integration of the measured angular distributions at energies where such measurements were made. The total cross section (σ) is greater than 4π times the differential cross section at 90° [$4\pi\sigma(90^\circ)$] by 8% at $E_{3\text{He}} = 2.0$ MeV, and by only 1% at $E_{3\text{He}} = 0.3$ MeV. The ratio $\sigma/4\pi\sigma(90^\circ)$ varies smoothly and slowly with energy. At energies where no angular distributions were measured, the total cross sections were obtained from $4\pi\sigma(90^\circ)$ and the interpolated (or extrapolated) value of the ratio $\sigma/4\pi\sigma(90^\circ)$. The variation of σ with center-of-momentum energy is shown in Fig. 7. The cross-section factor $S(E_{c.m.})$ was calcu-

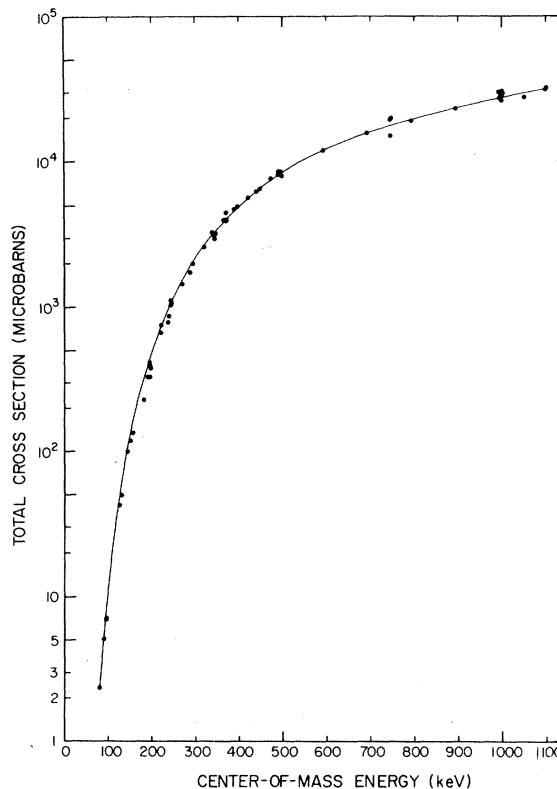


FIG. 7. ${}^3\text{He}({}^3\text{He}, 2p){}^4\text{He}$ total cross sections as a function of the center-of-momentum energy. The solid line is a guide to the eye.

lated from $\sigma(E_{c.m.})$ using the defining formula¹³

$$S(E_{c.m.}) = \sigma(E_{c.m.}) \times E_{c.m.} \times \exp\left(\frac{4.860}{E_{c.m.}^{1/2}}\right),$$

$E_{c.m.}$ in MeV.

Figure 8 shows the measured cross-section factors as a function of the c.m. energy. Total errors, including both counting statistics and estimated systematic errors, are shown at a few points. The figure also shows the cross-section factors as calculated from the measurements of Good, Kunz, and Moak,³ of Bacher and Tombrello,^{4,6} and of Neng-Ming *et al.*⁵ The cross-section factors of the present experiment were fitted to the function

$$S(E_{c.m.}) = S_0 + S_0' E_{c.m.}$$

by a standard least-squares routine over different ranges of energies. For $E_{c.m.} < 500$ keV, $S_0 = (5.0_{-0.4}^{+0.6})$ MeV b and $S_0' = (-1.8 \pm 0.5)$ b. The errors indicated in S_0 and S_0' include both statistical and systematic errors in the measured total cross section, as well as uncertainties in the bombarding energy. These errors have been discussed in Ref. 11. The data of Bacher and Tombrello⁶ give $S_0 = 5.4 \pm 0.5$ MeV b and $S_0' = -1.8 \pm 0.5$ b, and thus agree within the quoted errors.

All the cross-section factors measured in this work ($0.08 < E_{c.m.} < 1.1$ MeV) are well represented by the formula

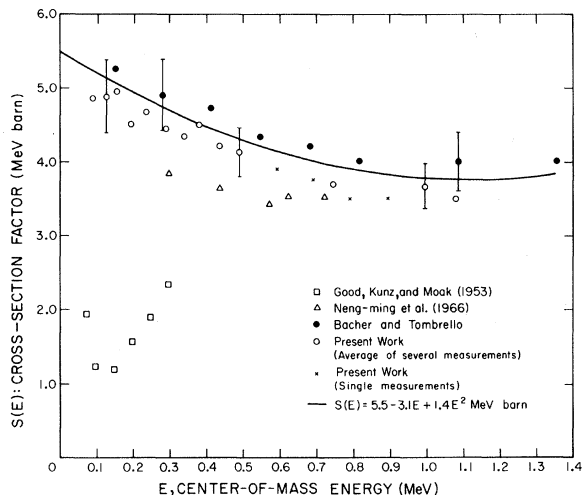


FIG. 8. ${}^3\text{He}({}^3\text{He}, 2p){}^4\text{He}$ cross-section factors as a function of center-of-momentum energy. Error bars indicated are typical, include statistical and estimated systematic errors in both measured total cross sections and center-of-momentum energy. Solid line is the curve $S(E_{c.m.}) = 5.5 - 3.1E_{c.m.} + 1.4E_{c.m.}^2$, which gives the best quadratic representation of the data of the present work and the data of Bacher and Tombrello.

$$S(E_{c.m.}) = S_0 + S_0' E_{c.m.} + \frac{1}{2} S_0'' E_{c.m.}^2,$$

with $S_0 = 5.2$ MeV b, $S_0' = -2.8$ b, and $S_0'' = 2.4$ b MeV^{-1} . However, the parameters that give a good fit to the experimental data are not unique (χ^2 has a shallow minimum in parameter space) because the variation in $S(E)$ is not very large compared with the errors in the measured $S(E)$. The combined data of the present work and of Bacher and Tombrello can be represented by the parameter values $S_0 = 5.5$ MeV b, $S_0' = -3.1$ b, and $S_0'' = 2.8$ b MeV^{-1} . The $S(E)$ as given by this latter set of parameters is shown as a solid line in Fig. 8.

IV. DISCUSSION

The results of Good, Kunz, and Moak³ are in serious disagreement with the present work. Their cross-section factor decreases rapidly from a value of 2.4 MeV b at $E_{c.m.} = 300$ keV to 1.2 MeV b at $E_{c.m.} = 150$ keV. Below this energy the cross-section factor increases sharply. This discrepancy is attributed to incomplete information on the distribution of ${}^3\text{He}$ in their target. The measurements of Neng-Ming *et al.*⁵ are in general agreement with the measurements reported here. The values of the cross-section factors agree within the combined errors of the two measurements, their $S(E_{c.m.})$ being systematically lower. They quote much larger errors in their energy determination than in the present work. This error is reflected in the values for $S(E_{c.m.})$.

Bacher and Tombrello⁶ have extended their measurements with a gas cell to $E_{c.m.} = 152$ keV. They minimized the uncertainty in the bombarding energy by experimentally measuring the energy loss at precisely the experimental energies. Their results are in very good agreement with the results given here. The absolute values of $S(E_{c.m.})$ agree within the limits of the combined errors,

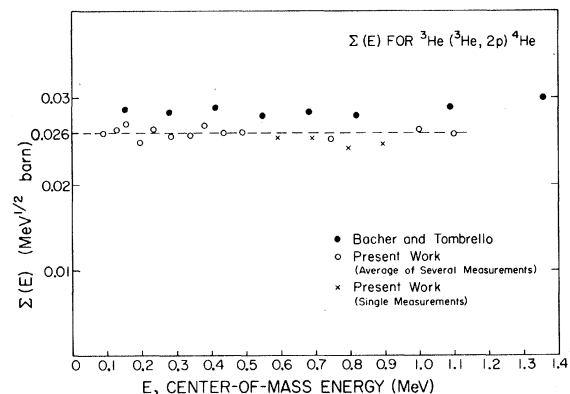


FIG. 9. $\Sigma(E)$, defined in text, as a function of the center-of-momentum energy. The dashed line denotes the average value of Σ for the present work.

their values being systematically higher by about 8%. The agreement in the energy variation of the cross-section factor is particularly impressive. The small systematic difference in the absolute values of $S(E_{\text{c.m.}})$ is not serious considering that the results have been obtained by two very different techniques.

Bacher and Tombrello⁸ observed that the reaction mechanism is not entirely sequential at energies below the Coulomb barrier, in contrast to its behavior at higher energies. The proton spectra exhibit less and less of the effects of the final-state interaction in the $({}^4\text{He} + p)$ system at lower energies; a different reaction mechanism appears to dominate at low energies. May and Clayton¹⁴ proposed a model in which a neutron from one of the ${}^3\text{He}$ nuclei "tunnels" to the other ${}^3\text{He}$ nucleus even when the two nuclei are outside the range of nuclear interaction. At low energies this mechanism might be expected to dominate over the other mechanisms which require a greater overlap of the ${}^3\text{He}$ nuclei, and may thus explain the change in shape of the proton spectra. May and Clayton calculated $S(E)$ for this reaction by considering a final-state interaction in the $(2p)$ system rather than in the $({}^4\text{He} + p)$ system. They obtained a negative value for S_0' as observed experimentally, but the calculated absolute value of S_0' was too small to fit the data.

Since the astrophysical cross section requires an extrapolation to energies below those at which measurements have been made, it is of interest to see whether the observed negative slope of $S(E)$ at low energies could be the result of factoring out a zero-radius s -wave penetration factor $(2\pi\eta e^{-2\pi\eta})$ from the total cross section. We define a quantity, $\Sigma(E)$, which should be independent of energy and is somewhat analogous to $S(E)$, by replacing the zero-radius s -wave penetration factor by finite-radius penetration factors according to the following expression for the cross section:

$$\sigma(E) = \frac{1 + \delta_{lj}}{2} \frac{\Sigma(E)}{\sqrt{E}} \left(\sum_l \omega_l \int_0^\infty P_l(r) T_l(r) r^2 dr \right),$$

where the first term on the right is chosen so as to give unity for reactions between identical particles. The $1/\sqrt{E}$ is the usual flux term and the density of final states is taken as independent of energy over the range of the present investigation, since the reaction has a large positive Q value. ω_l is the statistical weight for the relative motion of the interacting particles with angular momentum l . $P_l(r)$ is the probability per unit volume of finding the interacting particles at a separation r and $T_l(r)$ is the probability that the reaction occurs at a separation r in the l th partial wave.

A correct evaluation of the integral requires a

knowledge of the wave functions and is thus fairly complicated. As a simplification, we parametrize the integral as

$$\int_0^\infty P_l(r) T_l(r) r^2 dr = P_l(R_l) = \frac{1}{F_l^2(kR_l) + G_l^2(kR_l)},$$

where F_l and G_l are the regular and irregular Coulomb wave functions and the effective reaction radii R_l are adjustable parameters. Choosing different radius parameters for the different partial waves presumably takes into account the differences in the different $T_l(r)$. If we retain only the s -wave interaction and choose $R_0 = 0$, we obtain

$$\sigma(E) = \frac{\Sigma(E)}{\sqrt{E}} 2\pi\eta e^{-2\pi\eta} = \left[\sqrt{2} \pi Z_0 Z_1 \left(\frac{e^2}{\hbar c} \right) (\mu c^2)^{1/2} \Sigma(E) \right] \frac{1}{E} e^{-2\pi\eta}.$$

The quantity in square brackets is readily recognized as $S(E)$. It may be noted that, when comparing $S(E)$ for isobaric analog reactions, the $S(E)$ should be normalized by the factor $1/Z_0 Z_1$ before a comparison of the $S(E)$ values is made.

For the ${}^3\text{He}({}^3\text{He}, 2p){}^4\text{He}$ reaction we assume that only s waves and p waves are important at the low energies of these measurements and write

$$\sigma(E) = \frac{\Sigma(E)}{\sqrt{E}} [P_0(R_0) + 9P_1(R_1)],$$

or

$$\Sigma(E) = \sigma(E) \sqrt{E} [P_0(R_0) + 9P_1(R_1)]^{-1}.$$

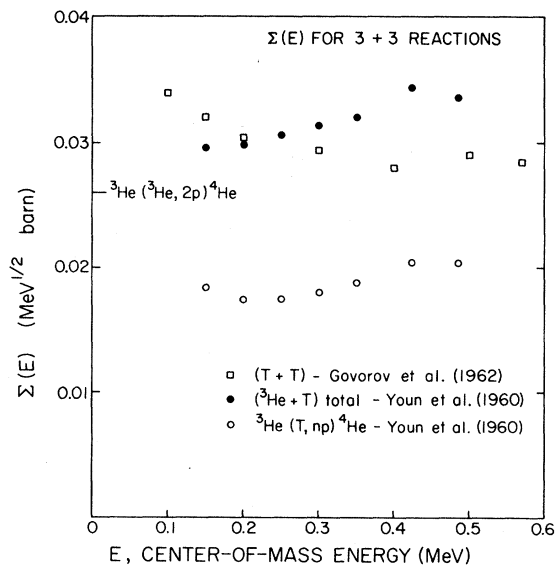


FIG. 10. $\Sigma(E)$ as a function of the center-of-momentum energy for the $T+T$ and ${}^3\text{He}+T$ reactions. The nearly constant value of Σ for the ${}^3\text{He}({}^3\text{He}, 2p){}^4\text{He}$ reaction of Fig. 9 is indicated on the ordinate.

The two free parameters R_0 and R_1 were adjusted to make $\Sigma(E)$ independent of energy. The best set of parameters to do this was $R_0 = 3.8$ fm and $R_1 = 3.0$ fm. The resulting $\Sigma(E_{c.m.})$ is shown in Fig. 9 as a function of $E_{c.m.}$. The average value of Σ is $0.026 \text{ MeV}^{1/2} \text{ b}$. Figure 9 also shows $\Sigma(E_{c.m.})$ calculated from the data of Bacher and Tombrello.

The same radius parameters were used to fit the data of Govorov *et al.*,¹⁵ on the mirror reaction ${}^3\text{H}({}^3\text{H}, 2n){}^4\text{He}$. The resulting $\Sigma(E_{c.m.})$ is approximately independent of energy (see Fig. 10) and the average value of Σ for this reaction is about $0.03 \text{ MeV}^{1/2} \text{ b}$, which is very close to the value obtained for ${}^3\text{He}({}^3\text{He}, 2p){}^4\text{He}$. The same prescription was also applied to the data of Youn *et al.*¹⁶ on the analog reaction ${}^3\text{He} + {}^3\text{H}$. In this reaction, the interacting particles are not identical and so we can have both singlet and triplet spin states for a given l . The statistical weights are therefore different and we have for ${}^3\text{He} + {}^3\text{H}$, assuming that the T_l 's are independent of spin,

$$\sigma(E) = \frac{1}{2} \frac{\Sigma(E)}{\sqrt{E}} [4P_0(R_0) + 12P_1(R_1)],$$

or

$$\Sigma(E) = \sigma(E) \sqrt{E} [2P_0(R_0) + 6P_1(R_1)]^{-1}.$$

The existence of a bound state in the (np) system complicates this reaction further. For this rea-

son the cross-section data for ${}^3\text{He}({}^3\text{H}, np){}^4\text{He}$ and the total reaction cross section for ${}^3\text{He} + {}^3\text{H}$ were fitted separately, with the same radius parameters as found for ${}^3\text{He} + {}^3\text{He}$. These are also shown in Fig. 10.

The resulting $\Sigma(E)$ is nearly independent of energy in each of these cases and the values of Σ agree to within $\pm 25\%$. By way of comparison, the experimentally determined value of S_0 for the reaction ${}^3\text{He}({}^3\text{He}, 2p){}^4\text{He}$ is about 30 times the S_0 value for the mirror reaction ${}^3\text{H}({}^3\text{H}, 2n){}^4\text{He}$. The S factors, normalized for the change in $Z_0 Z_1$ differ by a factor of about 7, which appears to be a result of using zero-radius penetrabilities.

The present study of the reaction ${}^3\text{He}({}^3\text{He}, 2p){}^4\text{He}$ yields a value of S_0 which is about 4.5 times larger than the value of $S_0 = 1.1 \text{ MeVb}$ adopted by Parker, Bahcall, and Fowler.¹ The effect of this change in S_0 is to reduce the originally predicted ${}^8\text{B}$ solar neutrino flux by a factor of about 2.

ACKNOWLEDGMENTS

We wish to thank Professor William A. Fowler for suggesting this problem and for his keen interest, help, and encouragement during the course of this work. Many illuminating discussions with Professor T. A. Tombrello, Professor C. A. Barnes, and Dr. A. D. Bacher are gratefully acknowledged.

*Work supported in part by the National Science Foundation Grant Nos. GP-28027, GP-19887.

†Present address: California State College, Los Angeles, California 90032.

¹P. D. Parker, J. N. Bahcall, and W. A. Fowler, *Astrophys. J.* **139**, 602 (1964).

²G. Shaviv, J. N. Bahcall, and W. A. Fowler, *Astrophys. J.* **150**, 725 (1967); R. Davis, Jr., *Phys. Rev. Letters* **12**, 303 (1964).

³W. M. Good, W. E. Kunz, and C. D. Moak, *Phys. Rev.* **83**, 845 (1951).

⁴A. D. Bacher and T. A. Tombrello, *Rev. Mod. Phys.* **37**, 433 (1965).

⁵W. Neng-Ming, V. N. Novatskii, G. M. Osetinskii, C. Nai-Kung, and I. A. Chepurchenko, *Yadern. Fiz.* **3**, 1064 (1966) [transl.: *Soviet J. Nucl. Phys.* **3**, 777 (1966)].

⁶A. D. Bacher and T. A. Tombrello, unpublished, as quoted in T. A. Tombrello, *Nuclear Research with Low-Energy Accelerators*, edited by J. B. Marion and D. M. Van Patter (Academic, New York, 1967).

⁷H. C. Winkler and M. R. Dwarakanath, *Bull. Am. Phys.*

Soc. **12**, 16, 1140 (1967).

⁸W. Whaling, in *Handbuch der Physik*, edited by S. Flügge (Springer, Berlin, 1958), Vol. 34, p. 193.

⁹L. C. Northcliffe, *Ann. Rev. Nucl. Sci.* **13**, 67 (1963).

¹⁰J. Cohen-Ganouna, M. Lambert, and J. Schmuev, *Nucl. Phys.* **40**, 82 (1963).

¹¹M. R. Dwarakanath, Ph.D. thesis, California Institute of Technology, 1968 (unpublished).

¹²H. Winkler and M. R. Dwarakanath, to be published.

¹³W. A. Fowler, G. R. Caughlan, and B. A. Zimmerman, *Ann. Rev. Astron. Astrophys.* **5**, 525 (1967).

¹⁴R. M. May and D. D. Clayton, *Astrophys. J.* **153**, 855 (1968).

¹⁵A. M. Govorov, L. Ka-Yeng, G. M. Osetinskii, V. I. Salatskii, and I. V. Sizov, *Zh. Eksperim. i Teor. Fiz.* **42**, 383 (1962) [transl.: *Soviet Phys.—JETP* **15**, 266 (1962)].

¹⁶L.-G. Youn, G. M. Osetinskii, N. Sodnom, A. M. Govorov, I. V. Sizov, and V. I. Salatskii, *Zh. Eksperim. i Teor. Fiz.* **39**, 225 (1960) [transl.: *Soviet Phys.—JETP* **12**, 163 (1961)].